



Products and bioenergy from the pyrolysis of rice straw via radio frequency plasma and its kinetics

Wen-Kai Tu^a, Je-Lung Shie^b, Ching-Yuan Chang^{a,*}, Chiung-Fen Chang^c, Cheng-Fang Lin^a, Sen-Yeu Yang^d, Jing T. Kuo^d, Dai-Gee Shaw^e, Yii-Der You^a, Duu-Jong Lee^f

^a Graduate Institute of Environmental Engineering, National Taiwan University, 71, Choushan Road, Taipei 10617, Taiwan

^b Department of Environmental Engineering, National I-Lan University, No. 1, Sec. 1, Shen-Lung Road, Ilan 26041, Taiwan

^c Department of Environmental Science and Engineering, Tung-Hai University, No. 181, Sec. 3, Taichung Harbor Road, Taichung 40704, Taiwan

^d Department of Mechanical Engineering, National Taiwan University, No. 1, Sec. 4, Roosevelt Road, Taipei 10617, Taiwan

^e Chung-Hua Institution for Economic Research, No. 75, Changsing Street, Taipei 10672, Taiwan

^f Department of Chemical Engineering, National Taiwan University, No. 1, Sec. 4, Roosevelt Road, Taipei 10617, Taiwan

ARTICLE INFO

Article history:

Received 21 June 2008

Received in revised form 25 September 2008

Accepted 26 September 2008

Available online 30 November 2008

Keywords:

Biomass waste
Radio frequency
Rice straw
Bioenergy
Pyrolysis

ABSTRACT

The radio frequency plasma pyrolysis technology, which can overcome the disadvantages of common pyrolysis methods such as less gas products while significant tar formation, was used for pyrolyzing the biomass waste of rice straw. The experiments were performed at various plateau temperatures of 740, 813, 843 and 880 K with corresponding loading powers of 357, 482, 574 and 664 W, respectively. The corresponding yields of gas products (excluding nitrogen) from rice straw are 30.7, 56.6, 62.5 and 66.5 wt.% with respect to the original dried sample and the corresponding specific heating values gained from gas products are about 4548, 4284, 4469 and 4438 kcal kg⁻¹, respectively, for the said cases. The corresponding combustible portions remained in the solid residues are about 64.7, 35, 28.2 and 23.5 wt.% with specific heating values of 4106, 4438, 4328 and 4251 kcal kg⁻¹ with respect to solid residues, while that in the original dried sample is 87.2 wt.% with specific heating value of 4042 kcal kg⁻¹. The results indicated that the amount of combustibles converted into gas products increases with increasing plateau temperature. The kinetic model employed to describe the pyrolytic conversion of rice straw at constant temperatures agrees well with the experimental data. The best curve fittings render the frequency factor of 5759.5 s⁻¹, activation energy of 74.29 kJ mol⁻¹ and reaction order of 0.5. Data and information obtained are useful for the future design and operation of pyrolysis of rice straw via radio frequency plasma.

© 2008 Published by Elsevier Ltd.

1. Introduction

The bioenergy from biomass, which is estimated to contribute about 10–14% of the primary energy supply of the world or about 38% of that of the developing countries (Bhattacharya et al., 2000; Mckendry, 2002), has a potential to provide a significant portion of the projected renewable energy provisions for the shortage of the oil. In general, the feasible characteristics of the biomass are: (1) high yield, (2) low energy input for plantation, (3) low cost, (4) least contaminants and (5) low nutrient requirements (Mckendry, 2002). Therefore, using the biomass wastes becomes a significant way to produce the bioenergy. Among the available biomass wastes, rice straw is one of the favorable waste sources of bioenergy, because it is the residue from the end use of the biomass prod-

ucts. The reutilization of rice straw not only saves the cost of disposal but also produces valuable bioenergy, achieving the goal of resources recovery and reuse. Taiwan locates in the subtropics and has excellent farming technology, thus producing abundant biomasses. However, this also results in a significant amount of agriculture wastes to be treated, with the rice straw contributing the most. In Taiwan, rice is one of the principal foods and the total annual generation of rice straw is about 1.4 million tons (Tu et al., 2008). The rice straw is difficult for burning in most existing combustion systems. The reasons are: (1) the fouling of deposits, (2) slag formation in furnaces and (3) accelerated corrosion (Bakker and Jenkins, 2003). Therefore, its common treatment is in-site burning for producing manure. However, the open burning is harmful to air quality and environment (Pütün et al., 2004).

Transform of the biomass wastes into bioenergy can be efficiently achieved applying thermochemical methods such as combustion, pyrolysis and gasification (Shie et al., 2001, 2002a; Chen et al., 2003b; Wu et al., 2003; Pütün et al., 2004). There are two

* Corresponding author. Tel./fax: +886 2 2363 8994.
E-mail address: cychang3@ntu.edu.tw (C.-Y. Chang).

main disadvantages of the pyrolysis and gasification of biomass wastes for producing gases of medium calorific value via the traditional thermolysis technology. These are: (1) the low gas yield, reducing the total energy value of gas and (2) the high content of tar in gas, causing the corroding problem of the gas collection equipment and increasing the need for the further treatment of the gas produced (Caldeira et al., 2002; Bridgwater, 2003; Chen et al., 2003a). The biomass treated via thermolysis yields the tar in the inferior temperatures and can undergo the cracking and re-polymerization in the superior temperatures above 673 K via secondary reactions (Ferdous et al., 2001; Chen et al., 2003b; Pütün et al., 2004). In order to provide the suitable fuel for spark ignition gas engines, the bio-fuel should be either gaseous or high quality liquid form (Mckendry, 2002). The common methods to overcome the above two disadvantages of the traditional thermolysis of biomass are adding catalysts and steam Shie et al., 2002b,c; Gullu, 2003; Atutxa et al., 2005; Demirbas, 2005; Waldner and Vogel, 2005). Worasuwannarak et al. (2007) applied the thermal gravimetry-mass spectrometry technique to study the pyrolysis behaviors of rice straw, yielding the pyrolysis products from rice straw at 873 K with compositions of char, H₂O, CO, CO₂, tar and sum of H₂ and CH₄ of 31, 25, 15, 15, 10 and 4 wt.%, respectively. Thus, other than H₂O, the CO and CO₂ are the dominant gas products, while H₂ and CH₄ are minor. Chen et al. (2003b) employed the catalysts to pyrolyze the rice straw, improving the gas yields at 1023 K with respect to the original un-dried sample containing about 10 wt.% H₂O from 36 wt.% without catalyst to 41, 42.2 and 46 wt.% with CaO, Na₂CO₃ and Cr₂O₃, respectively. However, even with the use of the catalyst of Cr₂O₃, the yield of tar is still as high as 10 wt.% at least. Pütün et al. (2004) reported that the feasible parameters for the pyrolysis of rice straw are with particle diameter of 20–40 mesh, gas flow of 200 mL min⁻¹, final temperature of 823 K and the steam velocity of 2.7 cm s⁻¹. Huang et al. (2008) employed the microwave-induced technology to pyrolyze the rice straw and yielded the H₂-rich fuel gas of nitrogen-free with H₂, CO₂, CO and CH₄ of 55, 17, 13 and 10 vol.%, respectively.

Application of a novel heating method via the radio frequency (RF) plasma is one of the feasible choices for overcoming the disadvantages of thermolysis using traditional heating methods (Tu et al., 2008). The RF plasma heating method, which is a capacitive dielectric heating method, employs the alternating current with high frequency and voltage to build up electro-magnetic field producing plasma to induce the target material resulting in the vigorous colliding, rubbing and thus self-heating. As the material is heated, pyrolysis occurs. The heating method using RF plasma has many advantages such as high heating rate, short heating time to reach setting temperature, low heat loss and low residual tar. Hence, this novel method can overcome the problems encountered in the traditional pyrolysis of biomass (Zhao et al., 2001; Bridgwater, 2003; Chen et al., 2003a; Merida et al., 2004; Yaman, 2004; Shie et al., 2008).

The plasma technologies for the thermolysis of biomass not only give high concentration of syngas, but also result in low concentration of tar in gas phase mostly below 10 mg Nm⁻³ as noted by Hlina et al. (2006). Low tar content in product obtained from RF plasma thermolysis also can be achieved because high energy species, such as electron, ion, atom and free radical produced from RF plasma can enhance the decomposition of tar (Tang and Huang, 2005a,b; Cheng et al., 2007). Tang and Huang (2005a,b) employed RF plasma pyrolysis with N₂ as carrier gas at 0.8 L min⁻¹ to treat the biomass of sawdust. The gas yield on average with respect to the original dried sample can reach 66 wt.% consisting of H₂, CO, CH₄, CO₂ and C₂ at an input power of 1800 W and an operating pressure of 5000 Pa (= 0.05 atm). The corresponding compositions of H₂, CO, CH₄, CO₂ and C₂ in the gas including N₂ are 3.88–11.06, 5.21–14.82, 1.38–2.48, 1.51–5.05 and 1.5–3.92 vol.%, respectively.

The total content of CO and H₂ in the gas products is 76 vol.% on a nitrogen-free basis, which can be used as syngas components.

2. Experimental section

The original RF plasma pyrolysis system (Tu et al., 2008) was modified adding the gas mixers, electromagnetic pulses stabilization device and effluent flow meter for the use in this study. The electromagnetic pulses stabilization device can stabilize the potential energy of the reactor when the RF plasma is produced and lead the electromagnetic pulses to the ground wire. The modified RF plasma pyrolysis system denoted as RFPT-N system is shown in Fig. 1. The RF plasma reactor consists of a quartz tube with outer diameter of 50 mm, wall thickness of 2 mm and length of 500 mm. The electrodes are two pieces of copper arcs with length of 320 mm, which are fixed around the outside of the quartz tube with a gap between two electrodes. The length of the RF plasma producing zone is about 320 mm. The electromagnetic pulses stabilization device stabilizes the potential energies of the upper and bottom stainless steel parts, hence preventing the interference of electromagnetic pulses on the digital monitors. Nitrogen with a purity of 99.99% was used as the working gas. Its flow rate through the drying tube was controlled via a mass flow controller of model 5850E from Brooks, Hatfield, PA, USA and checked by the effluent flow meter. In all experiments, nitrogen flow rate was kept at 200 mL min⁻¹. A pressure control valve is adopted to transfer the RFPT-N system from low-vacuum to atmosphere condition smoothly. A cold trap container with a volume of 3 L for controlling the outlet gas at a temperature of 298 ± 5 K is installed after the RF plasma pyrolysis reactor to collect the liquid products. In order to maintain a suitable degree of vacuum in the RFPT-N system, switch valves and vacuum meters of model CVG191GA from InstruTECH Inc., Bellmore, NY, USA, which are recorded by a vacuum monitor of Terranova model 906A from Duniway Stockroom Corp., Mountain View, CA, USA, are installed. Three digital thermometers of model TFC 305A, type K from Macro Fortunate Co., Taipei County, Taiwan were used to measure the temperatures at the inlet and inside of the RF plasma reactor, and the outlet of the cold trap. A RF plasma power supply of model QINTO3013 from Huettinger, Freiburg, Germany and an auto-matching box of model PFM3000A from Huettinger, Freiburg, Germany provide a maximum power of 2000 W and RF frequency of 13.56 MHz. The temperatures were controlled at various constant values from 740 ± 5 to 880 ± 5 K with the input powers at various constant values from 357 ± 2 to 664 ± 2 W at the pressure of 0.9 ± 0.04 torr. In this study, the RF plasma pyrolysis reactor was used for pyrolyzing the biomass waste of rice straw. In the batch experiments, the sample of rice straw was put in the crucible. After the completion of an experiment, the solid remained in the crucible was weighted. Three replicates were performed.

The effluent gas was vented to a fume hood for starting up and switched to the sampling port for collection using a sample bag as the experimental conditions of RFPT-N system were stable. When the run was finished, the nitrogen gas was kept flowing till the temperature of system was below 373 K.

The Brunauer–Emmett–Teller (BET) surface areas of samples were measured via the specific surface area analyzer of model ASAP2010 from Micromeritics, Norcross, GA, USA adopting gas adsorption method. Before analyzing, the sample was degassed at 378 K and 10⁻³ mmHg. It followed the nitrogen adsorption at 77 ± 0.5 K. The elements of C, H and N were analyzed via Heraeus CHN-O-Rapid analyzer from Heraeus Ltd., Hanau, Germany, and S and Cl via Tacussel Coulomax 78 automatic coulometric titrator from Tacussel, Lyons, France. The actual heating values of samples were measured using the adiabatic bomb calorimeter of model 150

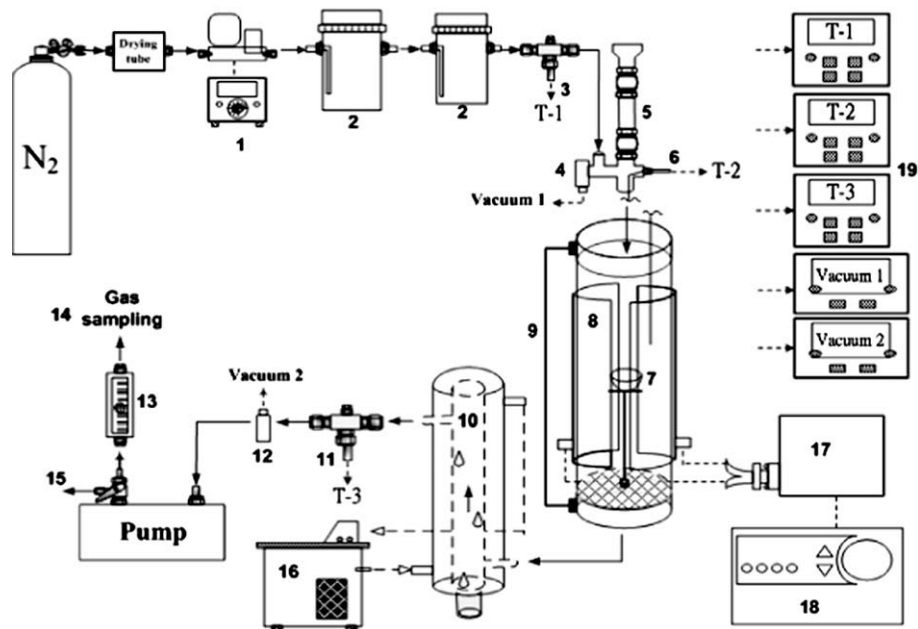


Fig. 1. The schematic diagram of the modified RF plasma pyrolysis (RFPT-N) system. 1. Mass flow rate controller. 2. Gas mixers. 3,6,11. Thermocouples. 4,12. Vacuum meters. 5. Pressure value. 7. Crucible and its support. 8. Copper electrodes. 9. Electromagnetic pulses stabilization device. 10. Condenser and liquid product collector. 13. Effluent flow meter. 14. Sampling port. 15. Vent to hood. 16. Circulating thermostat. 17. Auto-matching box. 18. RF plasma power supply. 19. Digital monitors.

Vacuum Flask Oxygen Bomb Calorimeter from Osaka Sanso Kogyo Ltd., Osaka, Japan, while the theoretic heating values of samples were calculated by Scheurer-Kestner formula (Srinivasa Reddy et al., 2005). The actual heating values can be estimated from the change of temperature in the adiabatic bomb calorimeter when the sample was burning and the detailed procedures can be referred to the standard test method for gross calorific value of coal and coke by the adiabatic bomb calorimeter (ASTM D2015, 2000; ASTM D3174-04, 2006).

The gaseous products of H_2 , CO and CO_2 were analyzed using gas chromatography-TCD of model 8900 from China Chromatography Co. Ltd., Taipei, Taiwan adopting column of #1-2390-U with dimensions of 15 ft \times 1/8 inch. The temperatures of injector, oven and detector were at 343, 368 and 343 K, respectively. The gaseous product of CH_4 was analyzed via gas chromatography-FID of model HP 6890 from Hewlett Packard Inc., California, USA using column of #115432 GS-Q with dimensions of 30 m \times 0.530 mm. The temperatures of injector, oven and detector were 373 K, 323 K for 10 min then raised to 523 K with heating rate of 10 K min^{-1} and 523 K, respectively. The gaseous products of total hydrocarbons were analyzed using gas chromatography-FID of model HP 5890 from Hewlett Packard Inc., California, USA with column of fused silica capillary tube with dimensions of 10 m \times 0.530 mm. The temperatures of injector, oven and detector were 423, 423 and 473 K, respectively. The detection limits of H_2 , CO, CO_2 , CH_4 and THCs are 2.2, 25.9, 21.9, 0.085 and 0.095 mg L^{-1} .

3. Results and discussion

3.1. Effects of loading power on the efficiency of pyrolysis of rice straw via RF plasma

The rice straw sample was exposed under the sunlight for 10 d, broken via spiral breaker, sieved into 30–40 mesh (0.6–0.425 mm) and dried in a recycle ventilation drier for 24 h at 378 K before use. The results of proximate and elemental analyses, heating value and BET surface area of rice straw with respect to the original dried sample are listed in Table 1. On the dry basis, the heating value

is as high as 4042 kcal kg^{-1} contributed by the high content of the combustibles of rice straw of 87.2 wt.%. The combustibles of rice straw are composed of 84 \pm 5 wt.% of volatile matter and 16 \pm 5 wt.% of fixed carbon (Chen et al., 2003b; Iranzo et al., 2004; Pütün et al., 2004; Worasuwannarak et al., 2007; Huang et al., 2008). Thus, the contents of volatile matter and fixed carbon of sample used in this study are 73.2 and 14 wt.%, respectively. The contents of C, H and O of rice straw are 41.8, 5.9 and 51.6 wt.% on dry basis, respectively, while those of nitrogen, sulfur and chloride are rare and can be neglected in the utilization of rice straw. The BET surface area is small with a value of 1.21 $m^2 g^{-1}$. The utilization of biomass for producing energy containing products also assists the reduction of CO_2 and SO_2 emissions for preventing the greenhouse effect and acid rain (Liang and Kozinski, 2000).

Table 1
Some properties of original rice straw^a used in this study^b.

Item	Value
<i>Proximate analysis (wt.%)</i>	
Moisture	0
Combustibles	87.2 (0.90) ^c
Ash	12.8 (1.15)
Heating value (kcal kg^{-1})	4042
<i>Elemental analyses (wt.%)</i>	
C	41.8 (0.01)
H	5.9 (0.06)
N	0.4 (0.01)
O	51.6 ^d
S	0.2 (0.02)
Cl	0.1
BET surface area ($m^2 g^{-1}$)	1.212

^a Dry basis.

^b Note that the samples used in the and present previous studies (Tu et al., 2008) were collected from different farmlands, showing slight difference in properties.

^c Numbers in parentheses are standard deviations (σ_{n-1}).

^d Balance.

The residual mass fraction (M) of rice straw with respect to the initial mass during pyrolysis is expressed on a normalized basis as

$$M = W/W_0 \quad (1)$$

where W and W_0 are the present and initial masses of sample, respectively.

The pyrolytic reaction of rice straw is significant in 550–650 K with two major reaction steps (Tu et al., 2008). Therefore, the plateau temperature for the pyrolysis of rice straw pyrolysis using RF plasma conducted in this study was set at the middle range of the second reaction step (740 ± 5 – 880 ± 5 K) to ensure an acceptable reaction rate of rice straw.

The effects of major system parameters on the performance of RF plasma pyrolysis of rice straw were examined. These parameters include loading power, reaction time and reaction temperature. The loading power can be measured online and recorded via the RF plasma power supply device. Maintaining the stable value of net pressure in the reactor can ensure the gas flowing through the plasma pyrolysis system with no leakage problem in experiments (Tu et al., 2008). The net pressure is the difference between the final pressure and the initial pressure under vacuum of 89 mtorr. For the followed pyrolysis experiments using RF plasma, the gas flow rate and net pressure of N_2 were set at 200 mL min^{-1} and 0.90 ± 0.04 torr, respectively.

Time variations of residual mass fraction and reaction temperature at various loading powers and plateau temperatures are shown in Fig. 2. The loading power used for the generation of RF plasma is equal to the input power minus reflected power. The input and reflected powers stand for the power supplied from the RF plasma power supply and the useless power producing the wasted electromagnetic wave from reflection, respectively. The results indicated that as the loading power increases from 357 to 664 W, the final value of residual mass fraction denoted as M_f at 45 min decreases from 69.3 to 33.5 wt.%, while the plateau temperature of plasma increases from 740 to 880 K. The rate of variation of residual mass fraction decreases while that of reaction temperature increases with the increase of loading power. The corresponding plateau temperatures at various loading powers are 740 K at 357 W, 813 K at 482 W, 843 K at 574 W and 880 K at 664 W, respectively. At loading powers of 357, 482, 574 and 664 W, the values of heating times t_{ST} to reach their corresponding setting temperatures T_{ST} , which are estimated as initial temperature T_0 plus 95% of the change of T_0 to the corresponding plateau temperatures, at 718, 787, 816 and 851 K are about 4.5, 4.17, 4 and 3.83 min with heating rates of 98, 124, 136 and 152 K min^{-1} , respectively. Thus, a higher loading power gives a higher plateau temperature with a shorter t_{ST} , resulting in a high heating rate which can be expressed as the following equations:

$$T_p \text{ (K)} = 0.4488P_{WL} + 585.97 \quad R^2 = 0.984 \quad (2)$$

$$\text{HR (K min}^{-1}\text{)} = 0.1722P_{WL} + 38.064 \quad R^2 = 0.9942 \quad (3)$$

where T_p , P_{WL} and HR are the plateau temperature, loading power and heating rate, respectively. The values of T_p and HR increase linearly with P_{WL} . Hence, HR can reach as high as about 152 K min^{-1} at P_{WL} of 664 W.

The average reaction rate r_{avg} before steady state can be estimated by further examination of the results of Fig. 2a. At various values of loading power, the values of residual mass fraction and time at steady state symbolized as M_{SS} and t_{SS} are about 69 ± 1 wt.% and 40 min at 357 W, 44 ± 1 wt.% and 30 min at 482 W, 37 ± 1 wt.% and 20 min at 574 W, and 33 ± 1 wt.% and 15 min at 664 W. The values of M_{SS} at t_{SS} are about equal to their corresponding final values of residual mass fraction M_f at 45 min,

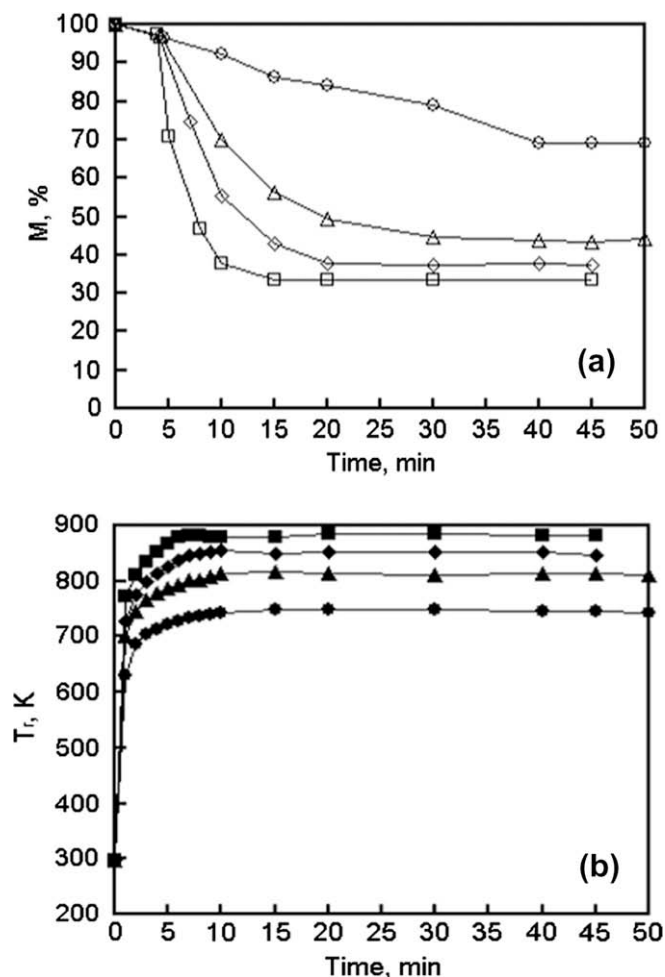


Fig. 2. Time variations of residual mass fraction (M) and reaction temperature (T_r) for the pyrolysis of rice straw via RF plasma method at various loading powers (P_{WL}) of 357 ± 2 (○), 482 ± 2 (△), 574 ± 2 (◇) and 664 ± 2 (□) W with plateau temperature (T_p) of 740 ± 5 (●), 813 ± 5 (▲), 843 ± 5 (◆) and 880 ± 5 (■) K, respectively. $P_{WL} = P_{WI} - P_{WR}$, P_{WI} , P_{WR} : Powers supplied and reflected. W_0 : 300 ± 10 mg. d_p : 0.425 – 0.6 mm. Carrier gas: N_2 . Q : 200 mL min^{-1} . P – P_0 : 0.9 ± 0.04 torr. T_0 : 298 ± 5 K. $M = W/W_0$. W , W_0 : Present and initial masses of sample. d_p : Sample size. Q : Flow rate of inlet carrier gas. P : Final pressure. P_0 : Initial pressure (89 m torr). T_0 : Initial or room temperature. (a) M vs. time, (b) T_r vs. time.

which are about 69.3, 43.4, 37.5 and 33.5 wt.%, respectively. As reaction temperature increases from T_0 to the setting temperature, the residual mass fraction only slightly reduces about 3.5, 2.9, 2.8 and 2.6 wt.% while retains 96.5, 97.1, 97.2 and 97.4 wt.% denoted as M_{ST} for the cases with loading power of 357, 482, 574 and 664 W, respectively, for further pyrolysis at various plateau temperatures. The corresponding decomposition efficiency of rice straw for further pyrolysis of M_{ST} to M_{SS} symbolized as $\eta_{ST/SS}$ is given as:

$$\eta_{ST/SS} = M_{ST} - M_{SS} \quad (4)$$

The values of $\eta_{ST/SS}$ are about 27.5, 53.1, 60.2 and 64.4 wt.%, respectively. The values of r_{avg} of RFPT-N system are estimated to be about 0.78, 2.06, 3.76 and $5.77 \text{ wt.}\% \text{ min}^{-1}$ at 357, 482, 574 and 664 W, respectively, using the following equation:

$$r_{avg} = \eta_{ST/SS} / (t_{SS} - t_{ST}) \quad (5)$$

Thus, a higher loading power gives higher decomposition efficiency and reaction rate.

Table 2

The fractions of products of solid remained, liquid and gas from the pyrolysis of rice straw via RFPT-N system at reaction time of 45 min and various plateau temperatures T_p applying various loading powers P_{WL} .

T_p (or P_{WL})	Solid remained (M_f) (wt.%)	Liquid products (wt.%)	Gas products (wt.%)
740 ± 5 K (or 357 ± 2 W)	69.3	0	30.7
813 ± 5 K (or 482 ± 2 W)	43.4	0	56.6
843 ± 5 K (or 574 ± 2 W)	37.5	0	62.5
880 ± 5 K (or 664 ± 2 W)	33.5	0	66.5

Initial mass of sample $W_0 = 300 \pm 10$ mg, diameter of sample $d_p = 0.425\text{--}0.6$ mm, flow rate of carrier gas $Q = 200$ mL min^{-1} of N_2 .

3.2. Fractions of products of solid, liquid and gas

Table 2 lists the fractions of the products of solid residue M , liquid and gas from the pyrolysis of rice straw via RFPT-N system at various loading powers P_{WL} and plateau temperatures T_p . The values are expressed with respect to the initial mass of dried sample. According to the studies of Lin and Lin (2006) and Tu et al. (2008), the major mineral constituents of rice straw are Si, Al, Na, Mg and Ca and the total content of oxide compounds of mineral matter is about 12.5 wt.% or 125,074.8 pp mw, which is close to that of ash of 12.8 wt.%.

From Table 2, the final residual mass fraction M_f at 45 min decreases as T_p and P_{WL} increase with M_f of 69.3, 43.4, 37.5 and 33.5 wt.% at T_p of 740, 813, 843 and 880 K, and P_{WL} of 357, 482, 574 and 664 W, respectively. No liquid products were collected from the RFPT-N system in this study. This may be due to the causes that only a small amount of rice straw less than 3.5 wt.% was decomposed in the heating stage with temperature rise and that the energy species generated via RF plasma can enhance the decomposition of tar and complex compounds if they were produced. Therefore, one can derive that the pyrolyzed part of rice straw is transformed to the gas products. Thus, the corresponding fractions of gas products are 30.7, 56.6, 62.5 and 66.5 wt.%, respectively. A higher loading power gives a higher plateau temperature and a larger amount of gas products.

3.3. Characteristics of gas products and solid residues

In order to examine the variation of concentration of gas products during the pyrolysis at various plateau temperatures T_p and loading powers P_{WL} , the gas was sampled at different time intervals with 4 min per interval such as 1–5 min, 6–10 min and 11–15 min till 41–45 min. Items of gas products analyzed included H_2 , CO, CH_4 , non-methane hydrocarbons (NMHCs) and the total hydrocarbons (THCs). The concentrations of NMHCs and THCs are expressed as CH_4 equivalence. The value of NMHCs is the difference between the values of THCs and CH_4 . Fig. 3 shows the instantaneous concentrations of gas products. The results indicated that the gas production is negligible in the heating period with temperature rise before reaching the setting temperature T_{ST} at time t_{ST} . After t_{ST} , gases are produced significantly as the pyrolysis proceeds vigorously at T_p with a higher T_p yielding more gases production as expected. The production of gases then reduces as the residual mass fraction M decreases approaching its final value M_f as shown in Fig. 2a. The maximum concentrations of various gas products appear earlier for higher T_p or P_{WL} . The characteristics of gas products measured via GC-FID indicated that the major constituents of NMHCs are hydrocarbons of $C_2\text{--}C_5$. The accumulated amounts of gas products $W_{G,Acc}$ in weight including H_2 , CO, CH_4 and NMHCs at various T_p or P_{WL} are shown in Fig. 4. At 45 min, the values of $W_{G,Acc}$ symbolled as $W_{G,Acc,f}$ at various P_{WL} of 357, 482, 574 and 664 W are 90.11, 147.2, 184.39 and 192.08 mg, respectively. More-

over, Fig. 4 shows that the linear gas producing rates of the middle portions are 6.01, 7.36, 7.38 and 7.68 mg min^{-1} at P_{WL} of 357, 482, 574 and 664 W, respectively. A higher P_{WL} can shorten the heating time for the production of gas products and give a higher T_p favourable to the pyrolytic reaction, thus resulting in a larger production of gas products with a higher producing rate. The yields and volume fraction contents of different component i denoted as $Y_{W,i}$ and V_i are listed in Table 3. As T_p increases from 740 to 880 K, sum of the yields of CO and H_2 of syngas increases greatly from 29.08 to 62.42 wt.%. Further, on nitrogen free basis, the volume fractions of syngas consisting of CO and H_2 are all above 97 vol.% for the four cases examined. Table 3 also gives the sums of yields of all gas products collected with values of 30.04, 49.07, 61.47 and 64.03 wt.% at T_p of 740, 813, 843 and 880 K, respectively. These values are close to the predicted values of 30.7, 56.6, 62.5 and 66.5 wt.% as listed in Table 2. Thus, the recoveries of gas products R_{CG} are about 98, 87, 98 and 96% for the cases with T_p of 740, 813, 843 and 880 K, respectively. Note that R_{CG} can also be estimated using the following equation:

$$R_{CG} = W_{G,Acc,f} / [W_0 \times (1 - M_f)] \quad (6)$$

Table 4 lists the BET surface area and element constituents of the solid residues at various T_p via RFPT-N system. The BET surface area increases from that of the original rice straw of 1.21 $\text{m}^2 \text{g}^{-1}$ to those of solid residues 2.11, 5.60, 5.86 and 6.50 $\text{m}^2 \text{g}^{-1}$ at T_p of 740, 813, 843 and 880 K, respectively. The feature of high heating rate HR of RFPT-N system is beneficial for reducing the formation of tar, while enhancing the production of gases of low molecular weights such as $C_2\text{--}C_5$ of hydrocarbons. However, the high HR of RFPT-N system may not provide enough time for the formation and development of pore structure of carbonaceous solid residues which although still contain about 42–50 wt.% of carbon. The common HR for the formation of pore structure of carbonaceous solid residues is about 5–20 K min^{-1} (Tsai et al., 2001). Thus, the BET surface area of the solid residues via RFPT-N system is inferior.

3.4. The kinetic model of combustible solid residues at constant temperature

Fig. 5 shows the time variation of residual mass fraction symbolled as M_{STF} after the heating time t_{ST} based on the total amount of mass pyrolyzed, which is denoted as W_{STF} , at various loading powers P_{WL} . The M_{STF} and W_{STF} are defined as

$$M_{STF} = (W - W_f) / W_{STF} \quad (7)$$

$$W_{STF} = W_{ST} - W_f \quad (8)$$

In Eqs. (7) and (8), W and W_f are the present and final masses of samples defined in the proceeding sections, W_{ST} is the mass of sample at t_{ST} or at the setting temperature T_{ST} . The values of M_{STF} are nearly constant after 35.5, 15.83, 11 and 6.17 min for the cases with P_{WL} of 357, 482, 574 and 664 W, respectively. The reaction rate equation is proposed for the M_{STF} as

$$dM_{STF}/d(t - t_{ST}) = -kM_{STF}^n \quad (9)$$

which gives

$$M_{STF} = [1 - (-n + 1)k(t - t_{ST})]^{1/(-n+1)} \quad (10)$$

where n is the reaction order and k is the reaction rate constant described by Arrhenius equation as $k = A \exp(-E_a/R_C T)$ with A , E_a and R_C representing the frequency factor, activation energy and universal gas constant (Huang et al., 2004). The best curve fittings render A of 5759.5 s^{-1} , E_a of 74.29 kJ mol^{-1} and n of 0.5. Fig. 5 compares the experimental data and the predicted results. The coefficients of determination R^2 are 0.973, 0.995, 0.997 and 0.963 for the cases with P_{WL} of 357, 482, 574 and 664 W, respectively. The

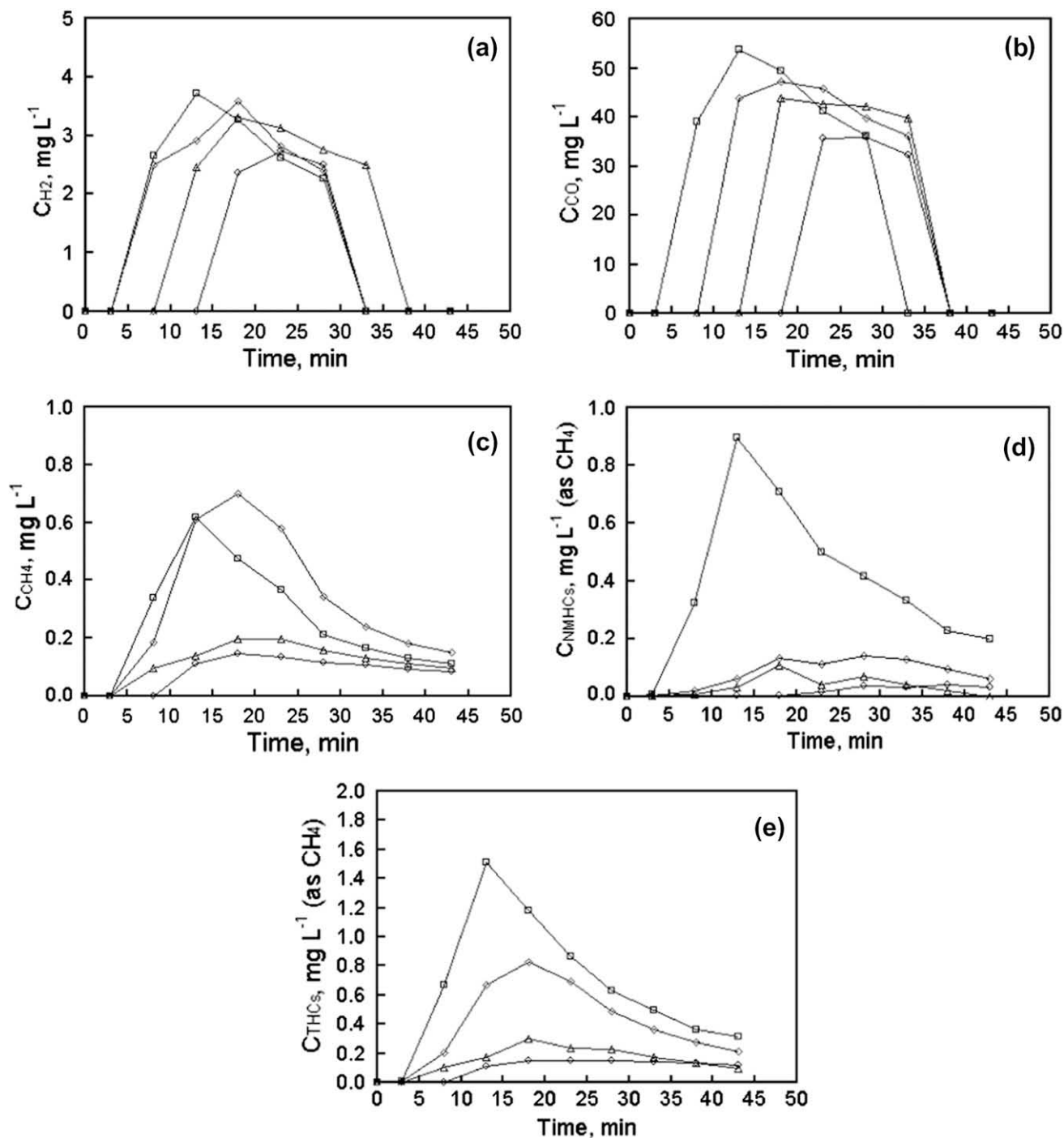


Fig. 3. Instantaneous concentrations of gas products for the pyrolysis of rice straw via RF plasma method at various P_{WL} . \circ , \triangle , \square , \square and other conditions are as those specified in Fig. 2. (a) H_2 , (b) CO , (c) CH_4 , (d) non-methane hydrocarbons (NMHCs), (e) total HCs (THCs).

good agreement between the two indicates that this model can be employed to describe the pyrolytic conversion of rice straw at constant temperatures.

3.5. The energy consumption and recovery and the heating values in the original sample and all products

The pyrolysis of rice straw via RF plasma can produce usable gas products not only as resources but also as energy with their corresponding specific heating values H_V . Table 5 lists the values of H_V of

gas and solid products obtained at various plateau temperatures T_p applying various loading powers P_{WL} . The specific heating values gained from the gas products denoted as $H_{V,G}$ are estimated via dividing the sum of all heating values of the corresponding combustible components by the total amount of gas products. The results are 4548, 4284, 4469 and 4438 $kcal kg^{-1}$ for the cases with T_p of 740, 813, 843 and 880 K, respectively.

The H_V of each residual solid symbolized as $H_{V,S}$ was calculated employing the Scheurer–Kestner formula, noted as S–K formula, using the element constituents in each residual solid listed in

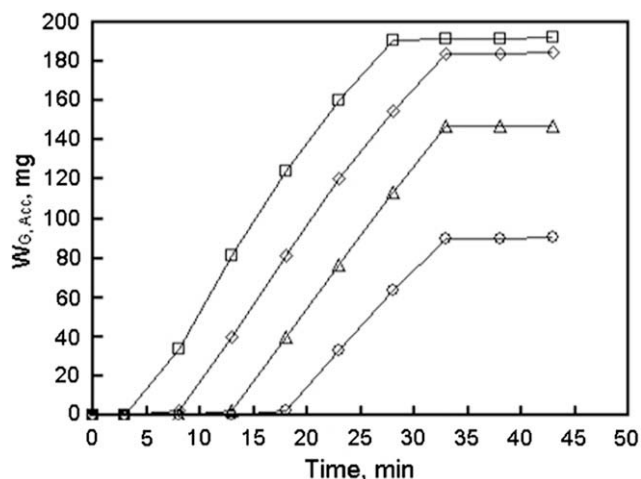


Fig. 4. Accumulated amounts of gas products ($W_{G,Acc}$) of H_2 , CO, CH_4 and NMHCs collected for the pyrolysis of rice straw via RF plasma method at various P_{WL} . (○), (△), (□), (◇) and other conditions are as those specified in Fig. 2.

Table 4. The actual $H_{V,S}$ of original rice straw was also measured using the adiabatic bomb calorimeter, giving the value of 4042 kcal kg^{-1} close to the theoretical $H_{V,S}$ of 4154 kcal kg^{-1} calculated with S–K formula. The less than 3% difference between these two values supports the validity of using the S–K formula to estimate the $H_{V,S}$ of solid samples. The S–K formula is as follows.

S–K formula:

$$H_{V,S} = 81 \left(C - \frac{3}{4} O \right) + 342.5H + 22.5S + 57 \times \left(\frac{3}{4} O \right) - 6(9H + W_{H_2O}) \quad (11)$$

in which, the C, O, H and S represent the percent contents of elements of sample in wt.% and W_{H_2O} is the moisture content of sample in wt.%. The numbers of 81, 342.5, 22.5 and 57 are the heats of combustion of C to CO_2 , H to H_2O , S to SO_2 and C to CO, respectively, in kcal kg^{-1} . The number of 6 is the heat of evaporation of water transfer to gaseous H_2O in kcal kg^{-1} . The numbers of 3/4 and 9 are the ratios of molecular weights of C to O and H_2O to H_2 , respectively. The masses of S and moisture content of the samples are low and can be neglected. Thus, also for the said cases, the corresponding combustible portions remained in the solid residues are 64.7, 35, 28.2 and 23.5 wt.% with $H_{V,S}$ of 4106, 4438, 4328 and 4251 kcal kg^{-1} with respect to the solid residues, respectively. The original dried sample contains 87.2 wt.% combustibles with $H_{V,S}$ of 4042 kcal kg^{-1} as already noted. The values of $H_{V,S}$ and $H_{V,G}$ of solid residues and gas products show small variation. However, the values of $H_{V,G} \times (W_0 - W_f)$ of gas products, representing the total heating values gained in gas products, are 418.9, 727.4, 838 and 885.3 cal for the corresponding cases, respectively, which increase

as T_p increases. The results indicated that the amount of combustibles converted into gas products increases with increasing T_p as expected.

The specific total heating value of solid and gas products denoted as $H_{V,T}$ increases from 4042 of original dried rice straw to about 4242, 4351, 4416 and 4375 kcal kg^{-1} at T_p of 740, 813, 843 and 880 K with corresponding P_{WL} of 357, 482, 574 and 664 W, respectively, as shown in Table 5. The total heating values noted as $H_{V,T} \times W_0$ are then calculated to be 1.21 kcal of original dried rice straw and 1.27, 1.31, 1.33 and 1.31 kcal for the pyrolytic products of rice straw respectively, as listed in Table 6. The energies consumed in the temperature-rising heating period of t_{ST} denoted as E_{ST} are about 0.08, 0.1, 0.12 and 0.13 kcal, and the corresponding energies consumed at the constant-temperature heating period at T_p to reach steady state symbolized as E_{TP} are about 0.64, 0.63, 0.46 and 0.37 kcal. Note that the amount of rice straw sample W_0 charged in the RFPT-N system for the pyrolysis experiments was about 0.3 g, while the allowable loading capacity W_a of the reactor is 85.12 g. Therefore, the values of E_{ST} and E_{TP} consumed by W_0 are computed as a fraction W_0/W_a of the energies input in the corresponding heating periods. The bulk density of rice straw in this study of 0.2 ± 0.01 g cm^{-3} was determined according to the procedures of Pendyal et al. (1999). The allowable batch amount of rice straw that can be treated in RFPT-N system is estimated considering the inner diameter of plasma reactor of 46 mm, length of plasma zone of 320 mm, bulk density of rice straw of 0.2 ± 0.01 g cm^{-3} and percent of usage of capacity of plasma reactor of 80 vol.%. This then gives the allowable loading capacity of rice straw of about 85.12 g. In obtaining $H_{V,T}$, E_{ST} and E_{TP} , the applicable equations are as follows.

$$H_{V,T} = H_{V,S} \times M_f + H_{V,G} \times (1 - M_f), \text{ in kcal } kg^{-1} \quad (12)$$

$$E_{ST} = [(P_{WL} \times t_{ST} + 60)/4.1868] \times (W_0/W_a), \text{ in cal} \quad (13)$$

$$E_{TP} = [P_{WL} \times (t_{SS} - t_{ST}) + 60]/4.1868 \times (W_0/W_a), \text{ in cal} \quad (14)$$

Table 6 lists the energy recoveries $R_{E,all}$ of the entire process including temperature-rising and constant-temperature heating periods for the pyrolysis of rice straw via RFPT-N system, giving 0.66, 0.68, 0.74 and 0.77 at P_{WL} of 357, 482, 574 and 664 W, respectively. The corresponding energy recoveries $R_{E,TP}$ of the process considering constant-temperature heating at the T_p are also presented in Table 6 with values of 0.69, 0.71, 0.8 and 0.83, respectively. The results indicated that the energy recovery increases as P_{WL} increases, suggesting that the pyrolysis via RF plasma is favorable applying a higher P_{WL} . In estimating $R_{E,all}$ and $R_{E,TP}$, the following equations are employed.

$$R_{E,all} = (H_{V,T} \times W_0) / [1.21 + (E_{ST} + E_{TP})] \quad (15)$$

$$R_{E,TP} = (H_{V,T} \times W_0) / (1.21 + E_{TP}) \quad (16)$$

Table 3
The yields ($Y_{W,i}$) and volume fractions of different components i (V_i) in the accumulated gas products from the pyrolysis of rice straw via RFPT-N system at reaction time of 45 min and various T_p applying various P_{WL} .

T_p (or P_{WL})	$Y_{W,CO}$ (wt.%)	Y_{W,H_2} (wt.%)	Y_{W,CH_4} (wt.%)	$Y_{W,NMHCs}$ (wt.%)	$Y_{W,G}^a$ (wt.%)	V_{CO} (vol.%)	V_{H_2O} (vol.%)	V_{CH_4} (vol.%)	V_{NMHCs} (vol.%)
740 ± 5 K (or 357 ± 2 W)	27.75 ^b	2.03 ^b	0.21 ^b	0.05 ^b	30.04 ^b	92.39 ^c (1.01) ^d	6.75 ^c (0.07) ^d	0.71 ^c (0.008) ^d	0.16 ^c (0.002) ^d
813 ± 5 K (or 482 ± 2 W)	44.9	3.78	0.3	0.09	49.07	91.51 (1.63)	7.70 (0.14)	0.61 (0.011)	0.18 (0.003)
843 ± 5 K (or 574 ± 2 W)	56.68	3.79	0.8	0.2	61.47	92.21 (2.06)	6.16 (0.14)	1.29 (0.029)	0.33 (0.007)
880 ± 5 K (or 664 ± 2 W)	58.54	3.88	0.65	0.96	64.03	91.43 (2.13)	6.06 (0.14)	1.01 (0.024)	1.51 (0.035)

^a $Y_{W,G} = Y_{W,CO} + Y_{W,H_2} + Y_{W,CH_4} + Y_{W,NMHCs}$.

^b With respect to the original dried sample.

^c On nitrogen free basis.

^d On nitrogen basis.

Table 4

The BET surface area denoted as A_{BET} and element analyses of solid residues from the pyrolysis of rice straw via RFPT-N system at reaction time of 45 min and various T_p applying various P_{WL} .

T_p (or P_{WL})	A_{BET} ($\text{m}^2 \text{g}^{-1}$)	C (wt.%)	H (wt.%)	N (wt.%)	O ^a (wt.%)	S (wt.%)	Cl (wt.%)
Original rice straw	1.21	41.8	5.9	0.4	51.6	0.2	0.1
740 ± 5 K (or 357 ± 2 W)	2.11	42.6	5.5	0.5	51.4	–	–
813 ± 5 K (or 482 ± 2 W)	5.60	49.8	4.3	0.8	45.1	–	–
843 ± 5 K (or 574 ± 2 W)	5.86	48.9	4.2	0.8	46.1	–	–
880 ± 5 K (or 664 ± 2 W)	6.50	49.4	3.8	0.7	46.1	–	–

–: Neglected and not measured.

^a Balance.

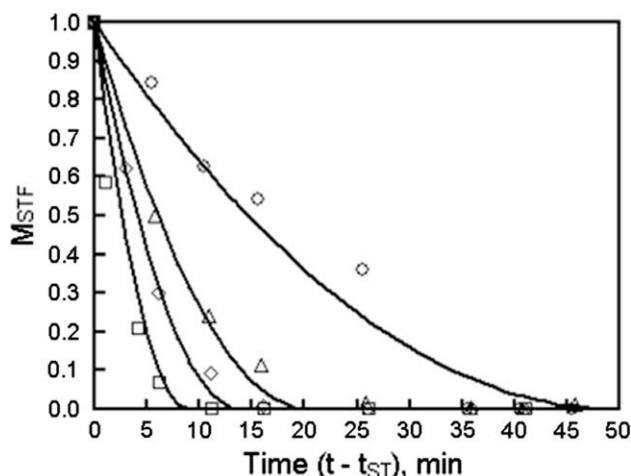


Fig. 5. Time variations of M_{STF} after t_{ST} for the pyrolysis of rice straw via RF plasma method at various P_{WL} . $M_f = 69.3, 43.4, 37.5$ and 33.5 , $t_{\text{ST}} = 4.5, 4.17, 4$ and 3.83 min, and $R^2 = 0.973, 0.995, 0.997$ and 0.963 for $P_{\text{WL}} = 357, 482, 574$ and 664 W, respectively. $n = 0.5$. Symbols and lines: Experimental data and prediction. M_{STF} : Residual mass fraction based on total amount of mass pyrolyzed, $= (W - W_f)/(W_{\text{ST}} - W_f)$. W, W_f : Present and final masses of samples. W_{ST} : Mass of sample at heating time t_{ST} reaching setting temperature. R^2 : Coefficient of determination. n : Reaction order. (○), (△), (□), (◇) and other conditions are as those specified in Fig. 2.

Table 5

The specific heating values (H_v) of original sample and all products from the pyrolysis of rice straw via RFPT-N system at reaction time of 45 min and various T_p applying various P_{WL} .

T_p (or P_{WL})	$H_{v,S}$ (kcal kg^{-1})	$H_{v,G}$ (kcal kg^{-1})	$H_{v,T}$ (kcal kg^{-1})
Original rice straw (actual)	4042	NA	4042
Original rice straw (theoretical)	4154	NA	4154
740 ± 5 K (or 357 ± 2 W)	4106	4548	4242
813 ± 5 K (or 482 ± 2 W)	4438	4284	4351
843 ± 5 K (or 574 ± 2 W)	4328	4469	4416
880 ± 5 K (or 664 ± 2 W)	4251	4438	4375

$H_{v,S}$ and $H_{v,G}$: Specific heating values of solid residues and gas products, respectively.

$H_{v,T}$: Specific total heating value of solid and gas products from pyrolysis, $= H_{v,S} \times M_f + H_{v,G} \times (1 - M_f)$.

$H_{v,T}$ of original rice straw: same as $H_{v,S}$.

$H_{v,\text{CO}}, H_{v,\text{H}_2}, H_{v,\text{CH}_4}$ and $H_{v,\text{NMHCs}} = 282.99, 285.84, 890.35$ and $890.35 \text{ kJ mol}^{-1} = 2413, 34136, 13291$ and $13291 \text{ kcal kg}^{-1}$.

NA: Not applicable.

Table 6

The energy consumption and recovery and heating values of all products from the pyrolysis of rice straw via RFPT-N system at reaction time of 45 min applying various P_{WL} .

P_{WL}	$H_{v,T} \times W_0$ (kcal)	E_{ST} (kcal)	E_{TP} (kcal)	$R_{E,\text{all}}$	$R_{E,\text{TP}}$
357 W	1.27	0.08	0.64	0.66	0.69
482 W	1.31	0.1	0.63	0.68	0.71
574 W	1.33	0.12	0.46	0.74	0.8
664 W	1.31	0.13	0.37	0.77	0.83

$H_{v,T}$: Specific heating value with unit in kcal kg^{-1} .

W_0 : Mass of sample, $= 0.3 \times 10^{-3} \text{ kg}$.

$H_{v,T} \times W_0$ of original rice straw: 1.21 kcal.

E_{ST} : Energy consumed in temperature-rising heating period of t_{ST} .

E_{TP} : Energy consumed at constant-temperature heating at T_p to reach steady state of solid residues.

$R_{E,\text{all}}$: Energy recovery ratio of the entire process including temperature-rising and constant-temperature heating periods as calculated using Eq. (15).

$R_{E,\text{TP}}$: Energy recovery ratio of the process considering constant-temperature heating at T_p as computed using Eq. (16).

4. Conclusions

The RFPT-N system overcomes the problem of tar formation during the pyrolysis of rice straw. In this system, a higher loading power gives a higher plateau temperature with a shorter heating time to reach setting temperature. The high heating rate of RF plasma can efficiently decompose the combustible solid to gas products of $\text{H}_2, \text{CO}, \text{CH}_4$ and low carbon hydrocarbons such as $\text{C}_2\text{--C}_5$. The production of gases increases as the pyrolysis is proceeded vigorously at a higher plateau temperature. Also, an increase in loading power increases the total heating value of the products of gas and solid residues.

The kinetic model employed to describe the pyrolytic conversion of rice straw at constant temperature agrees well with the experimental data. The frequency factor, activation energy and reaction order are $5759.5 \text{ s}^{-1}, 74.29 \text{ kJ mol}^{-1}$ and 0.5, respectively. The obtained data and information are useful for the rational operation and design of pyrolysis of rice straw via RF plasma.

The energy recovery from the pyrolysis of rice straw via RFPT-N system increases with increasing loading power. In practical, the rice straw can be pre-treated via pelletization to prepare the refuse derived fuel before being charged into the reactor. This can increase the density of rice straw pellet and the capacity of loading, enhancing the energy utilization efficiency.

Acknowledgement

We express our sincere thanks to the National Science Council of Taiwan for the financial support, under the contract No. NSC95-2218-E-002-035.

Appendix Notations. and abbreviations

A	Frequency factor, s^{-1}
BET	Brunauer–Emmett–Teller
d_p	Diameter of sample, mm
E_a	Activation energy, kJ mol^{-1}
E_{ST}	Energy consumed in temperature-rising heating period of t_{ST} , kcal
E_{TP}	Energy consumed at constant-temperature heating at T_p to reach steady state of solid residues, kcal
H_v	Specific heating value, kcal kg^{-1}
$H_{v,G}$	H_v of gas products, kcal kg^{-1}
$H_{v,S}$	H_v of solid residues, kcal kg^{-1}

$H_{V,T}$	Specific total heating value of solid and gas products, = $H_{V,S} \times M_f + H_{V,G} \times (1 - M_f)$, kcal kg ⁻¹
HR	Heating rate, K min ⁻¹
k	Reaction rate constant, = $A \exp(-Ea/R_G T)$, s ⁻¹
M	Residual mass fraction defined in Eq. (1), = W/W_0 , -
M_f	Final value of M at 45 min, -
M_{SS}	Value of M at t_{SS} , -
M_{ST}	Value of M at T_{ST} or t_{ST} , -
M_{STF}	Residual mass fraction after t_{ST} based on W_{STF} , = $(W - W_f)/W_{STF}$, -
NMHCS	Non-methane hydrocarbons
n	Reaction order, -
P	Final pressure, Torr
P_0	Initial pressure, Torr
P_{WI}	Input power, W
P_{WL}	Loading power, = $P_{WI} - P_{WR}$, W
P_{WR}	Reflected power, W
Q	Flow rate of carrier gas, mL min ⁻¹
R^2	Coefficient of determination, = $1 - [\sum(y_e - y_p)^2 / \sum(y_e - y_{e,Average})^2]$, -
R_{CG}	Recovery of gas products estimated using Eq. (6), wt.%
$R_{E,all}$	Energy recovery ratio of the entire process including temperature-rising and constant-temperature heating periods as calculated using Eq. (15), -
$R_{E,TP}$	Energy recovery ratio of the process considering constant-temperature heating at T_p as computed using Eq. (16), -
R_G	Universal gas constant, 0.008314 kJ K ⁻¹ mol ⁻¹
RF	Radio frequency
RFPT	RF Plasma pyrolysis (thermolysis)
RFPT-N	Modified RFPT
t_{avg}	Average reaction rate during t_{ST} to t_{SS} as calculated using Eq. (5), wt.% min ⁻¹
T_p	Plateau temperature, K
T_r	Reaction temperature, K
T_{ST}	Setting temperature, = $T_0 + 0.95 (T_p - T_0)$, K
T_0	Initial or room temperature, K
THCS	Total hydrocarbons
t_H	Heating time, min
t_{SS}	Heating time to reach steady state, min
t_{ST}	Heating time to reach T_{ST} , min
V_i	Volume fraction of component i in the accumulated gas products, vol.%
W	Present mass of sample, mg
W_0	Initial mass of sample, mg
W_a	Allowable loading capacity of the reactor, g
W_f	Final mass of sample after 45 min reaction, mg
$W_{G,Acc}$	Accumulated amount of gas products, mg
$W_{G,Acc,f}$	Values of $W_{G,Acc}$ at 45 min, mg
W_{H2O}	Moisture content of sample, wt.%
W_{ST}	Mass of sample at T_{ST} or t_{ST} , mg
W_{STF}	Total amount of mass pyrolyzed after t_{ST} , = $W_{ST} - W_f$, mg
$Y_{w,i}$	Yield of component i in the accumulated gas products with respect to the original dry solid sample, wt.%
y_e	Value of experimental data
y_p	Predicted value
$\eta_{ST/SS}$	Decomposition efficiency for further pyrolysis of M_{ST} to M_{SS} as computed using Eq. (4), wt.%

References

- ASTM D2015, 2000. Standard Test Method for Gross Calorific Value of Coal and Coke by the Adiabatic Bomb Calorimeter, American Society for Testing and Materials, Conshohocken, PA, USA.
- ASTM D3174-04, 2006. Standard Test Method for Ash in the Analysis Sample of Coal and Coke from Coal, American Society for Testing and Materials, Conshohocken, PA, USA.

- Atutxa, A., Aguado, R., Gayubo, A.G., Olazar, M., Bilbao, J., 2005. Kinetic description of the catalytic pyrolysis of biomass in a conical spouted bed reactor. *Energy and Fuels* 19, 765–774.
- Bakker, R.R., Jenkins, B.M., 2003. Feasibility of collecting naturally leached rice straw for thermal conversion. *Biomass and Bioenergy* 25, 597–614.
- Bhattacharya, S.C., Salam, P.A., Sharma, M., 2000. Emissions from biomass energy use in some selected Asian countries. *Energy* 25, 169–188.
- Bridgwater, A.V., 2003. Renewable fuels and chemicals by thermal processing of biomass. *Chem. Eng. J.* 91, 87–102.
- Caldeira, M.I.K., Benford, G., Criswell, D.R., Green, C., Herzog, H., Jain, A.K., Khesghi, H.S., Lackner, K.S., Lewis, J.S., Lightfoot, H.D., Manheimer, W., Mankins, J.C., Mauel, M.E., Perkins, L.J., Schlesinger, M.E., Volk, T., Wigley, T.M.L., 2002. Advanced technology paths to global climate stability: energy for a greenhouse planet. *Science* 298, 981–987.
- Chen, G., Andries, J., Luo, Z., Spliethoff, H., 2003a. Biomass pyrolysis/gasification for product gas production: the overall investigation of parametric effects. *Energy Convers. Mgmt.* 44, 1875–1884.
- Chen, G., Andries, J., Spliethoff, H., 2003b. Catalytic pyrolysis of biomass for hydrogen rich fuel gas production. *Energy Convers. Mgmt.* 44, 2289–2296.
- Cheng, H.H., Chen, S.S., Wu, Y.C., Ho, D.L., 2007. Non-thermal plasma technology for degradation of organic compounds in wastewater control: a critical review. *J. Environ. Eng. Manage.* 17, 427–433.
- Demirbas, A., 2005. Relationship between Initial moisture content and the liquid yield from pyrolysis of saw dust. *Energy Sources* 27, 823–830.
- Ferdous, D., Dalai, A.K., Bej, S.K., Thring, R.W., Bakshi, N.N., 2001. Production of H₂ and medium Btu gas via pyrolysis of lignins in a fixed-bed reactor. *Fuel Process Technol.* 70, 9–26.
- Gullu, D., 2003. Effect of catalyst on yield of liquid products from biomass via pyrolysis. *Energy Sources* 25, 753–765.
- Hlina, M., Hrabovsky, M., Kopecky, V., Konrad, M., Kavka, T., Skoblja, S., 2006. Plasma gasification of wood and production of gas with low content of tar. *Czechoslovak J. Phys.* 56, B1179–B1184.
- Huang, H.C., Chang, C.Y., Chen, Y.H., Shie, J.L., Lin, J.P., Wu, C.H., 2004. Resources recovery of waste rayon by pyrolysis: kinetics study. *J. Chin. Inst. Chem. Engrs.* 35, 623–632.
- Huang, Y.F., Kuan, W.H., Lo, S.L., Lin, C.F., 2008. Total recovery of resources and energy from rice straw using microwave-induced pyrolysis. *Bioresour. Technol.* 99, 8252–8258.
- Iranzo, M., Cañizares, J.V., Roca-Perez, L., Sainz-Pardo, I., Mormeneo, S., Boluda, R., 2004. Characteristics of rice straw and sewage sludge as composting materials in Valencia (Spain). *Bioresour. Technol.* 95, 107–112.
- Liang, X.H., Kozinski, J.A., 2000. Numerical modeling of combustion and pyrolysis of cellulosic biomass in thermogravimetric systems. *Fuel* 79, 1477–1486.
- Lin, K.L., Lin, C.Y., 2006. Feasibility of using ash from sludge incineration as raw materials for eco-cement. *J. Environ. Eng. Manage.* 16, 39–46.
- Mckendry, P., 2002. Energy production from biomass (part 1): overview of biomass. *Bioresour. Technol.* 83, 37–46.
- Merida, W., Maness, P.C., Brown, R.C., Levin, D.B., 2004. Enhanced hydrogen production from indirectly heated, gasified biomass, and removal of carbon gas emissions using a novel biological gas reformer. *Int. J. Hydrogen Energy* 29, 283–290.
- Pendyal, B., John, M.M., Marshalf, W.E., Ahmedna, M., Rao, R.M., 1999. The effect of binders and agricultural by-products on physical and chemical properties of granular activated carbons. *Bioresour. Technol.* 68, 247–254.
- Püttin, A.E., Apaydm, E., Püttin, E., 2004. Rice straw as a bio-oil source via pyrolysis and steam pyrolysis. *Energy* 29, 2171–2180.
- Shie, J.L., Chang, C.Y., Lin, J.P., Lee, D.J., Wu, C.H., 2001. Thermal degradation kinetics of oil sludge in the presence of carbon dioxide. *J. Chin. Inst. Environ. Eng.* 11, 307–316.
- Shie, J.L., Chen, Y.H., Chang, C.Y., Lin, J.P., Lee, D.J., Wu, C.H., 2002a. Thermal pyrolysis of polyvinyl alcohol and its major products. *Energy and Fuels* 16, 109–118.
- Shie, J.L., Chang, C.Y., Lin, J.P., Lee, D.J., Wu, C.H., 2002b. Effect of feeding oxygen fraction on gas emission and solid residue from oxidative thermal treatment of oil sludge. *J. Chin. Inst. Environ. Eng.* 12, 65–76.
- Shie, J.L., Lin, J.P., Chang, C.Y., Lee, D.J., Wu, C.H., 2002c. Use of calcium compounds as additives for oil sludge pyrolysis. *J. Chin. Inst. Environ. Eng.* 12, 363–371.
- Srinivasa Reddy, M., Basha, S., Joshi, H.V., Sravan Kumar, V.G., Jha, B., Ghosh, P.K., 2005. Modeling the energy content of combustible ship-scraping waste at Alang-Sosiya, India, using multiple regression analysis. *Waste Manage.* 25, 747–754.
- Shie, J.L., Chang, C.Y., Tu, W.K., Tang, Y.C., Liao, J.K., Tzeng, C.C., Li, H.Y., Yu, Y.J., Kuo, C.H., Chang, L.C., 2008. Major products obtained from plasma torch pyrolysis of sunflower-oil cake. *Energy and Fuels* 22, 75–82.
- Tang, L., Huang, H., 2005a. Plasma pyrolysis of biomass for production of syngas and carbon adsorbent. *Energy and Fuels* 19, 1174–1178.
- Tang, L., Huang, H., 2005b. Biomass gasification using capacitively coupled RF plasma technology. *Fuel* 84, 2055–2063.
- Tsai, W.T., Chang, C.Y., Wang, S.Y., Chang, C.F., Chien, S.F., Sun, H.F., 2001. Preparation of activated carbons from corn cob catalyzed by potassium salts and subsequent gasification with CO₂. *Bioresour. Technol.* 78, 203–208.
- Tu, W.K., Shie, J.L., Chang, C.Y., Chang, C.F., Lin, C.F., Yang, S.Y., Kuo, J.T., Shaw, D.G., Lee, D.J., 2008. Pyrolysis of rice straw using radio-frequency plasma. *Energy and Fuels* 22, 24–30.
- Waldner, M.H., Vogel, F., 2005. Renewable production of methane from woody biomass by catalytic hydrothermal gasification. *Ind. Eng. Chem. Res.* 44, 4543–4551.

- Worasuwannarak, N., Sonobe, T., Tanthapanichakoon, W., 2007. Pyrolysis behaviors of rice straw, rice husk, and corncob by TG-MS technique. *J. Anal. Appl. Pyrol.* 78, 265–271.
- Wu, C.H., Chang, C.Y., Tseng, C.H., Lin, J.P., 2003. Pyrolysis product distribution of waste toilet paper in a laboratory-scale TGA reactor. *J. Chin. Inst. Environ. Eng.* 13, 67–76.
- Yaman, S., 2004. Pyrolysis of biomass to produce fuels and chemical feed stocks. *Energy Convers. Mgmt.* 45, 651–671.
- Zhao, Z.L., Huang, H.T., Wu, C.Z., Li, H.B., Chen, Y., 2001. Biomass pyrolysis in an argon/hydrogen plasma reactor. *Chem. Eng. Tech.* 24, 197–199.